Part I day 3. Reminder: Overview

Intrinsic galaxy alignment (IA)

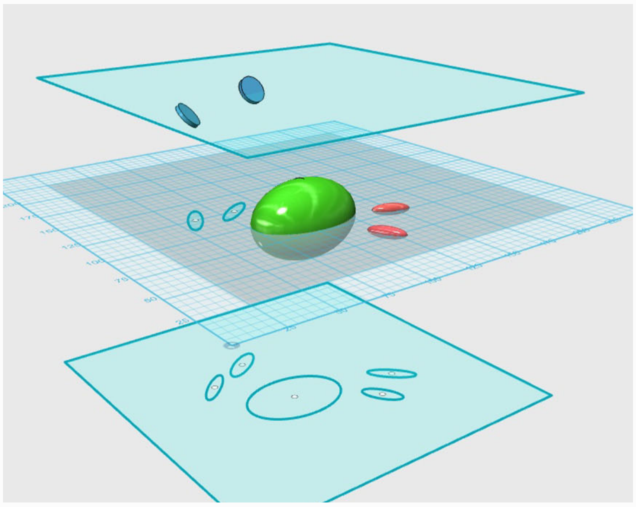

(Joachimi et al. 2015)

Galaxy shapes are correlated with surrounding tidal density field, due to coupling of spins for spiral galaxies, tidal stretching for elliptical galaxies.
Shape of galaxies is sum of shear (G) and intrinsic (I) shape (remember $\varepsilon \approx \varepsilon^{\rm s} + \gamma$).
So, with intrinsic alignment, the correlation of galaxy shapes is not only shear-shear (GG), but also intrinsic-intrinsic (II) and shear-intrinsic (GI; (Hirata & Seljak 2004)).

Contamination to cosmic shear at ~ 1 - 10%.
Need to model galaxy formation.

IA measurement: Ellipticity - density correlations

With (spectroscopic) data measure γ_t around massive galaxies (= centres of halos): shape - density correlations.

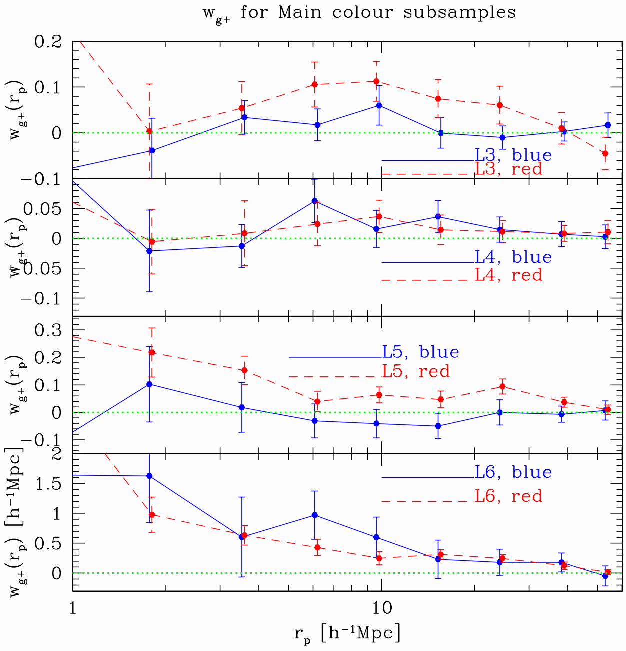

(Hirata et al. 2007)

IA measurement: Ellipticity - ellipticity correlations

With photometric data measure sum of GG, GI, and II.

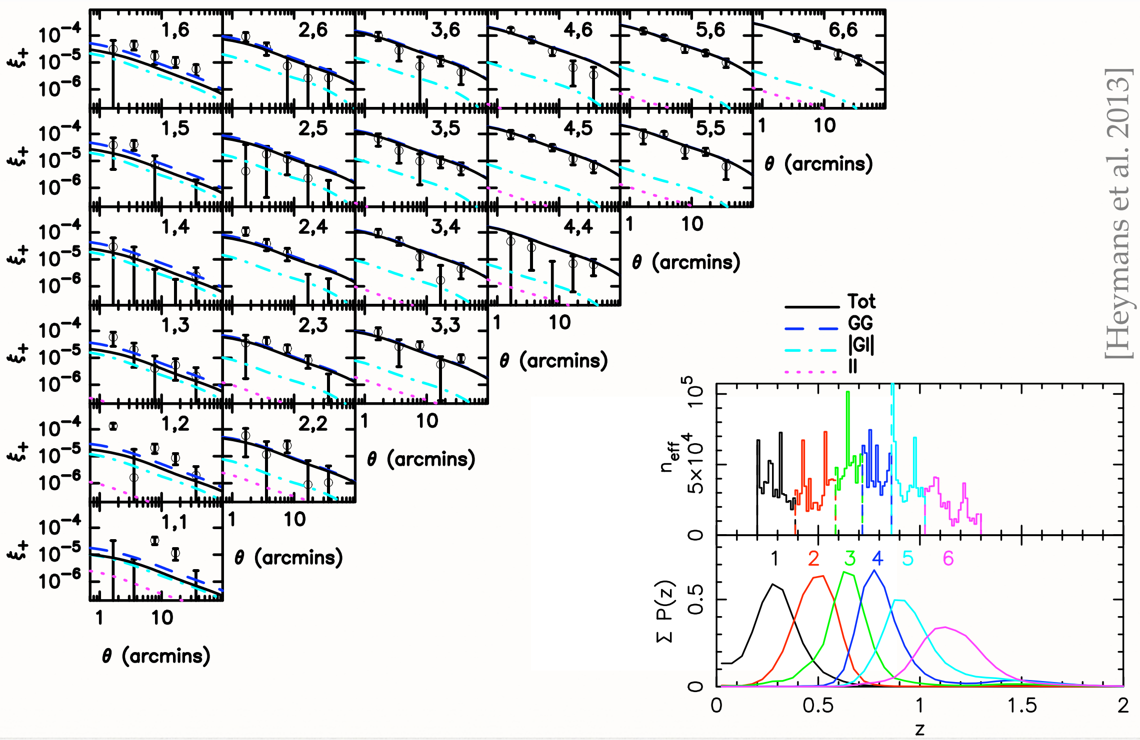

[Heymans et al. 2013]

IA constraints

Simple intrinsic alignment model:
Galaxy ellipticity linearly related to tidal field
[Hirata & Seljak 2004, Bridle & King 2007].

One free amplitude parameter A, fixed z-dependence.

A = 1: reference IA model.
A = 0: no IA

$A_{\rm late} = 0.18^{+0.83}_{-0.82}$

$A_{\rm early} = 5.15^{+1.74}_{-2.32}$

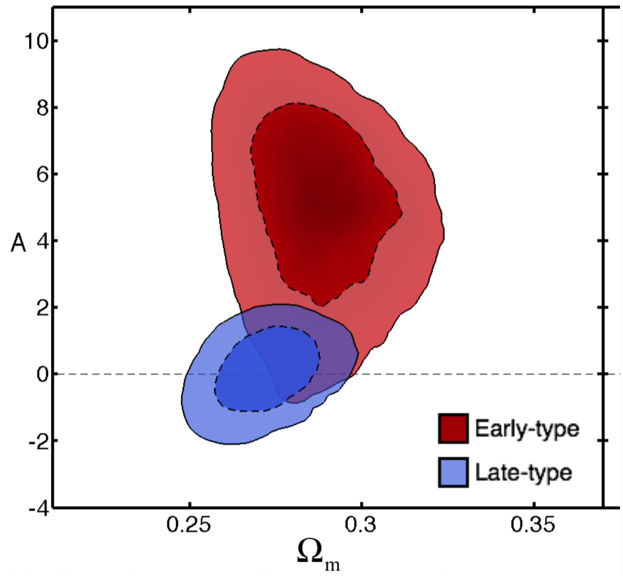

[Heymans et al. 2013]

Baryons in the LSS

On small (halo) scales, dark-matter only models do not correctly reproduce clustering:

- $R \sim 1$ - 0.1 Mpc: gas pressure $\rightarrow$ suppression of structure formation, gas distribution more diffuse wrt dm
- $R < 0.1$ Mpc ($k > 10$/Mpc): Baryonic cooling, AGN+SN feedback $\rightarrow$ condensation of baryons to form stars and galaxies, increase of density, stronger clustering

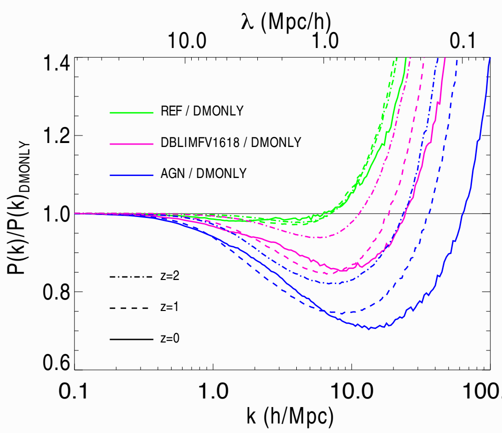

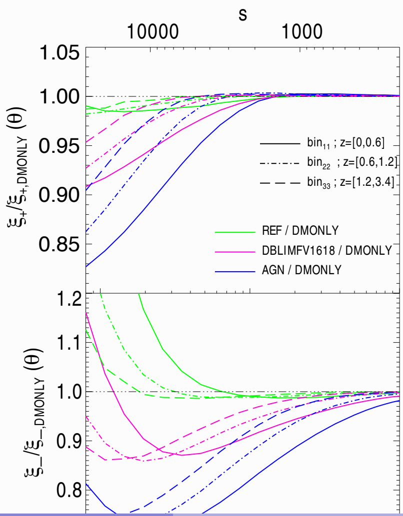

CFHTLS/CFHTlenS

Groundbreaking for weak cosmological lensing:

- MegaCam 1 deg^2 fov (@ 3.6m CFHT)
- Multiple optical bands → photometric redshifts, tomography
- Large team (> 20; led by Yannick Mellier, Catherine Heymans, Ludovic van Waerbeke), thorough testing, multiple pipelines
- Public release of all data and lensing catalogues (`www.cfhtlens.org`)

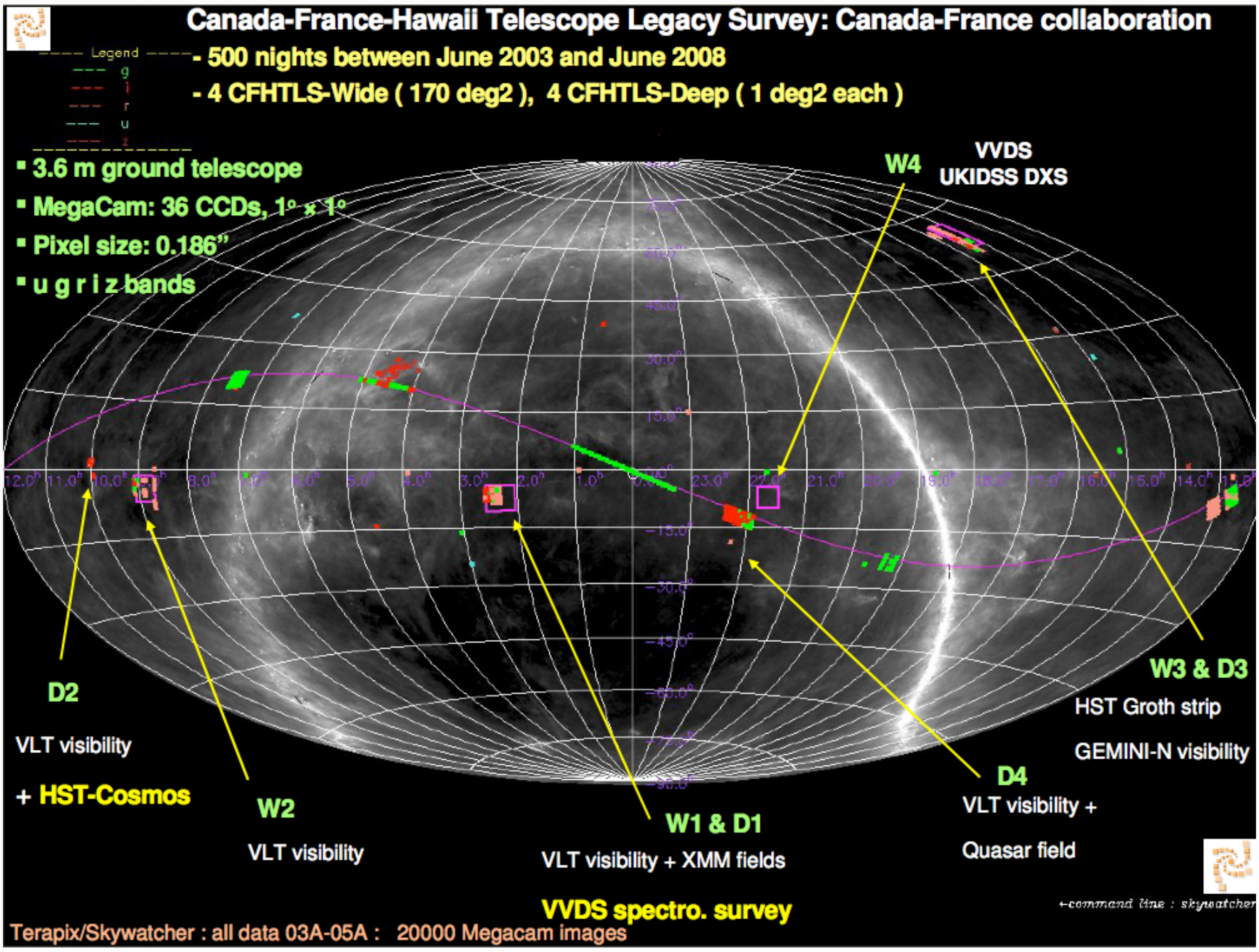

CFHTlenS cosmological constraints

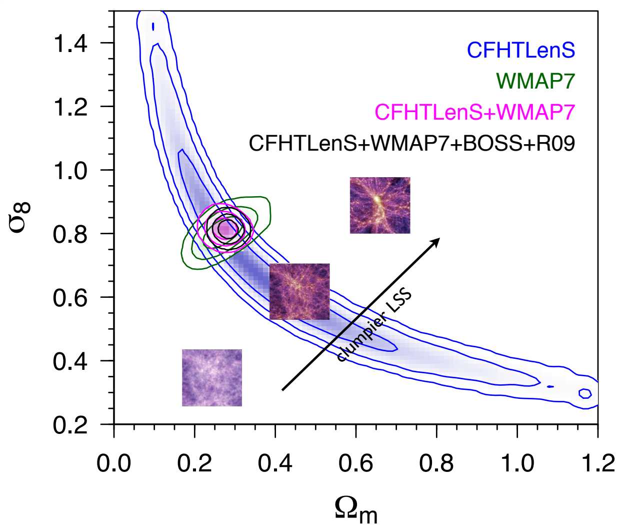

2D lensing
(Kilbinger et al. 2013)

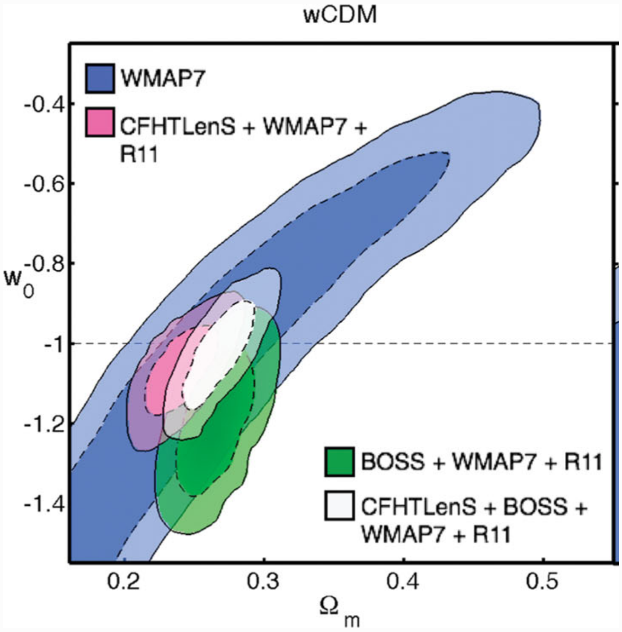

6-bin tomography
(Heymans et al. 2013)

CFHTlenS modified gravity

$$ds^2 = -(1+2\varphi)dt^2 + (1-2\phi)a^2 d\vec{x}^2$$

time dilation — spatial curvature

- Gravitational potential as experienced by galaxies:

$$\nabla^2\varphi = 4\pi G a^2 \bar\rho\delta \left[1+\mu\right] \qquad \mu(a) \propto \Omega_\Lambda(a)$$

- Gravitational potential as experienced by photons:

$$\nabla^2(\varphi+\phi) = 8\pi G a^2 \bar\rho\delta \left[1+\Sigma\right] \qquad \Sigma(a) \propto \Omega_\Lambda(a)$$

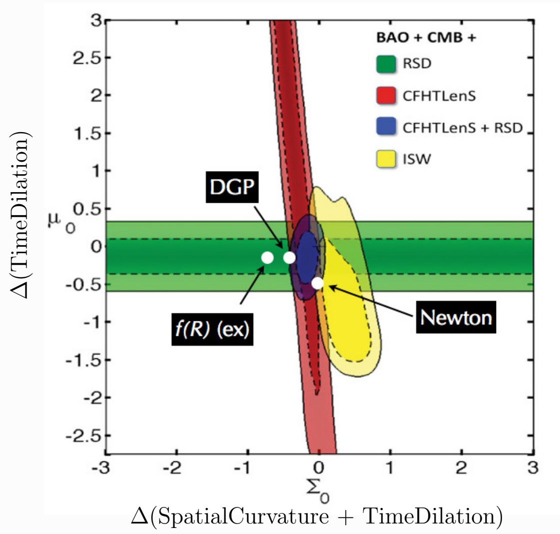

2-bin tomography
(Simpson et al. 2013)

DES — Dark Energy Survey

- Dedicated new camera: DECam, 3 deg^2 fov, weak lensing as main science goal
- @ 4m class Blanco telecsope on Cerro Tololo, Chile
- $5,000$ deg^2 when completed
- Large coverage in other wavelength (e.g. SPT)
- Ongoing survey, published results (2016) from Science Verification Data, 139 deg^2 = 3% of final area, but nominal depth and filters

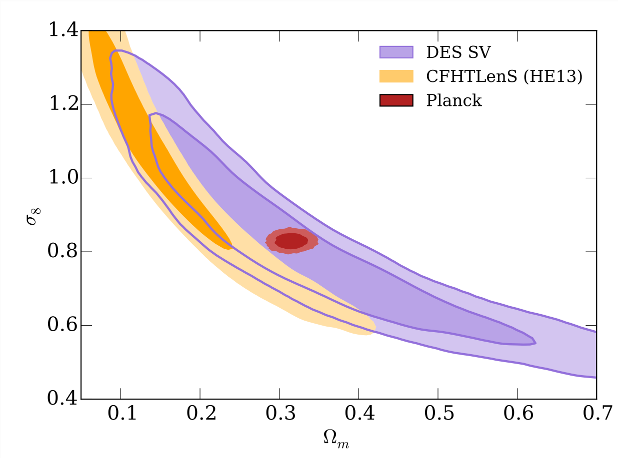

(The Dark Energy Survey Collaboration et al. 2016)

KiDS

- $1,500$ deg^2 in four optical (+ 5 IR) bands
- New camera (OmegaCAM 1 deg^2 fov) and telescope (2.6 m VST), long delay
- Compared four different redshift estimation methods

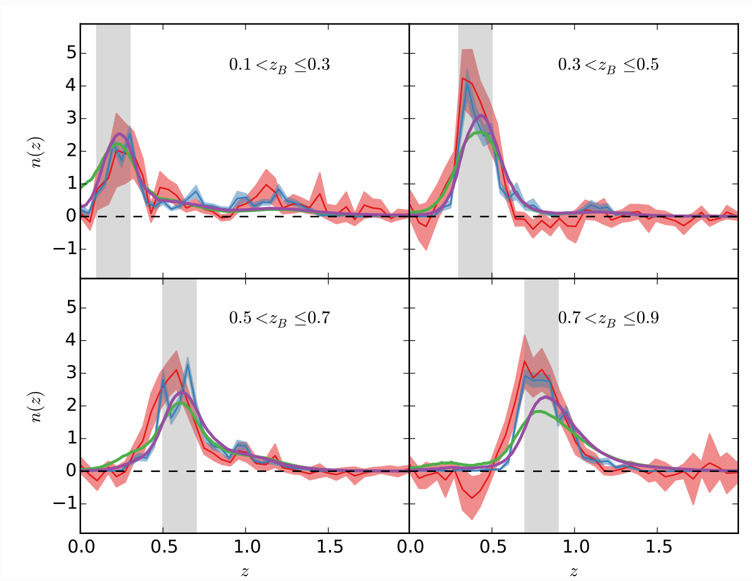

(Hildebrandt et al. 2017)

KiDS

Very thorough weak-lensing analysis, including:

- $n(z)$ errors
- IA, baryonic effects
- Shear calibration
- Non-Gaussian covariance
- Blinded analysis

(Hildebrandt et al. 2017)

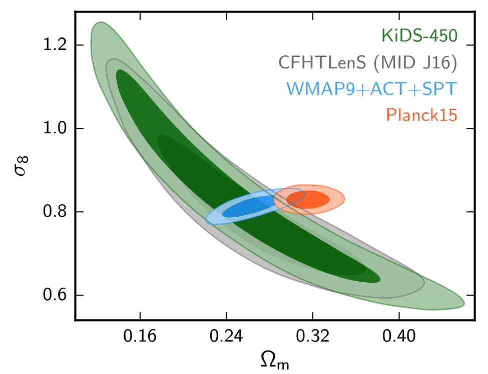

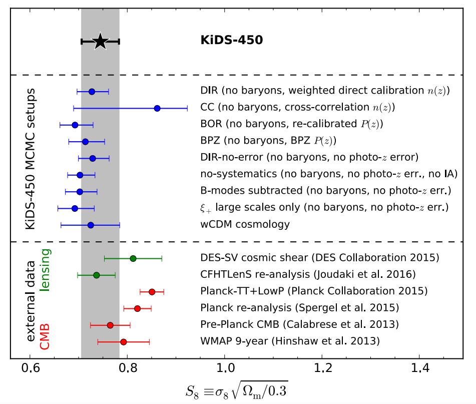

Summary

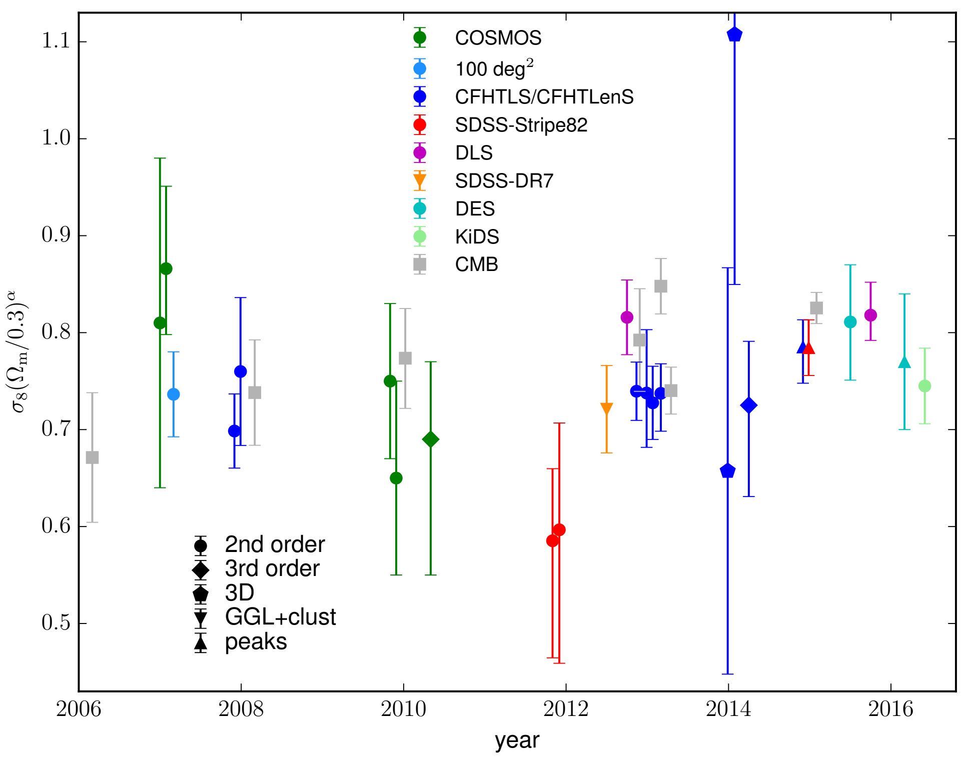

Discrepancy with Planck?

- Maybe not (2 - 3σ). However, also discrepancy of CMB C_ℓ's with SZ cluster counts.
- Additional physics, e.g. massive neutrinos? Not sufficient evidence.
- WL systematics? (E.g. shear bias, baryonic uncertainty on small scales.) KiDS say not likely.

The Euclid mission

Why is Euclid so special and challenging?
Increase of factor 100 in data volume compare to current surveys!
Few Million to few 100 Million galaxies.

For 2PCF: Naive increase of $n_{\rm correl}$ by $10,000$!

Comparison with Planck:
Planck all-sky, pixel size $\sim$ 7 arc min.
Euclid 1/3 sky, pixel size $\sim$ typical angular distance between galaxies $\sim$ arc sec.
Factor 10^5 more pixels!

Weak-lensing resolution

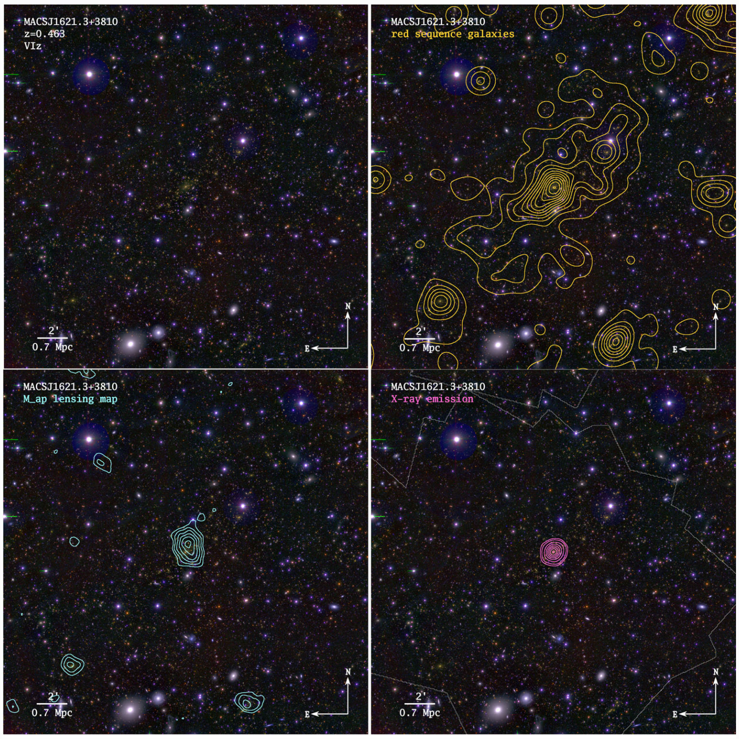

(von der Linden et al. 2014) — MACS_J1621+3810, ground-based data, $n_{\rm gal} = 2.5 \ldots 25 \; \rm arcmin^{-2}$

Weak-lensing resolution

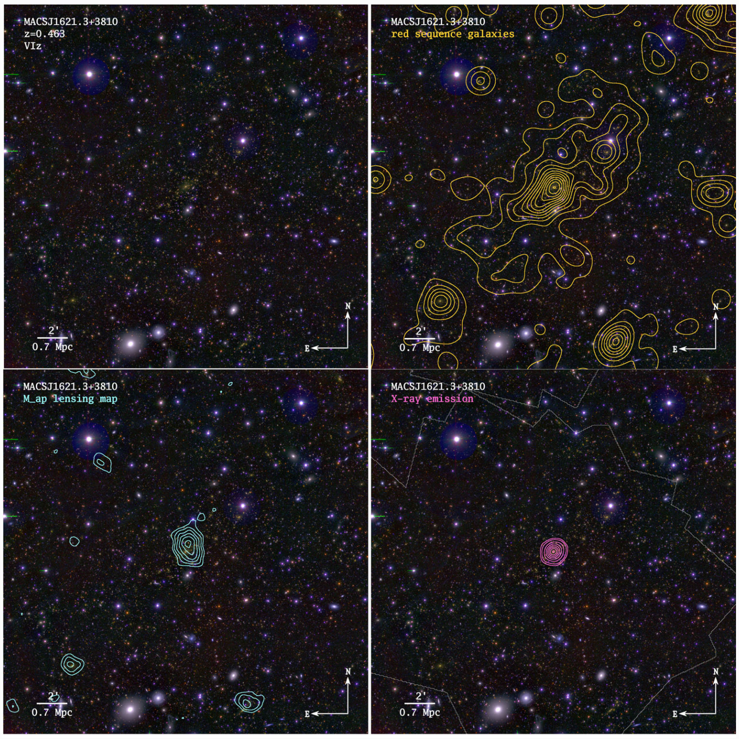

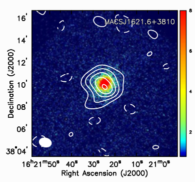

(Bonamente et al. 2012) — X- and SZ

Weak-lensing resolution

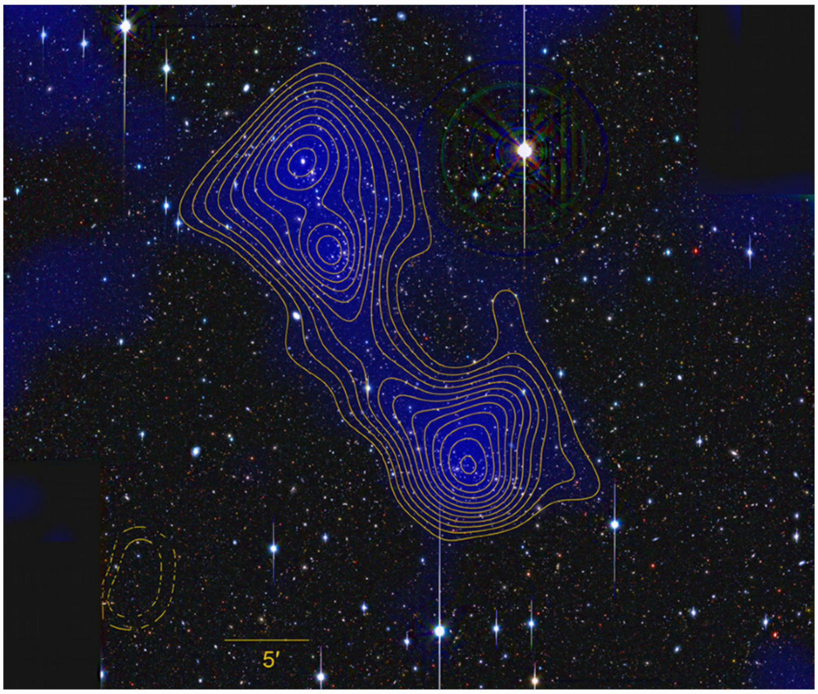

A 222/223, filament between clusters (Dietrich et al. 2012)

Mass maps from CFHTLenS

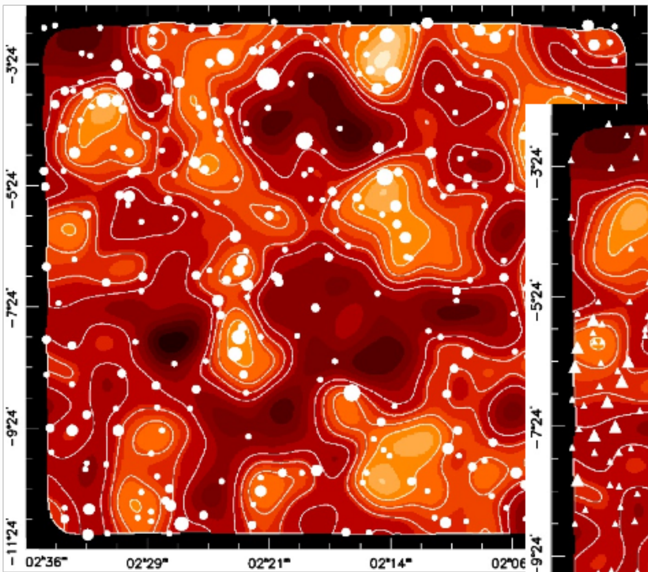

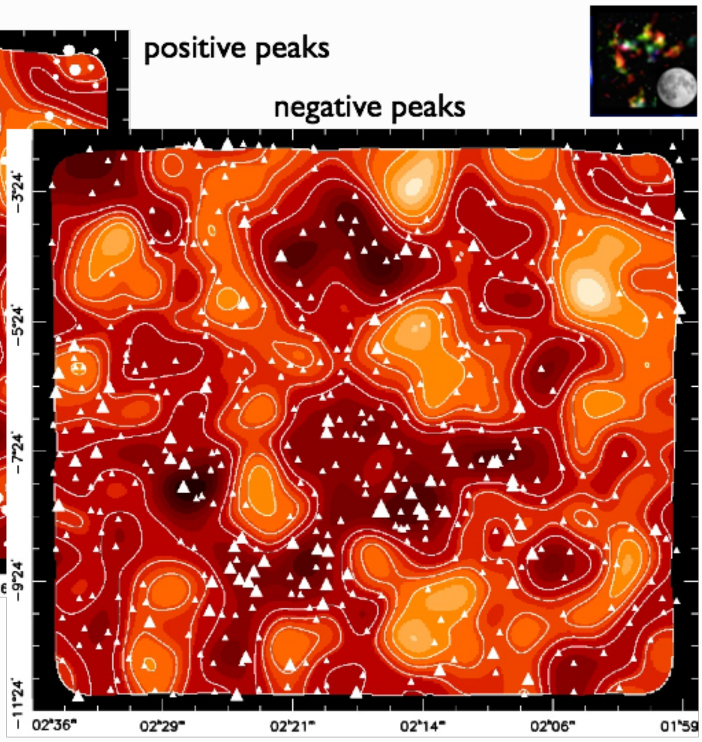

CFHTLenS W1
(van Waerbeke et al. 2013a)

Euclid imaging

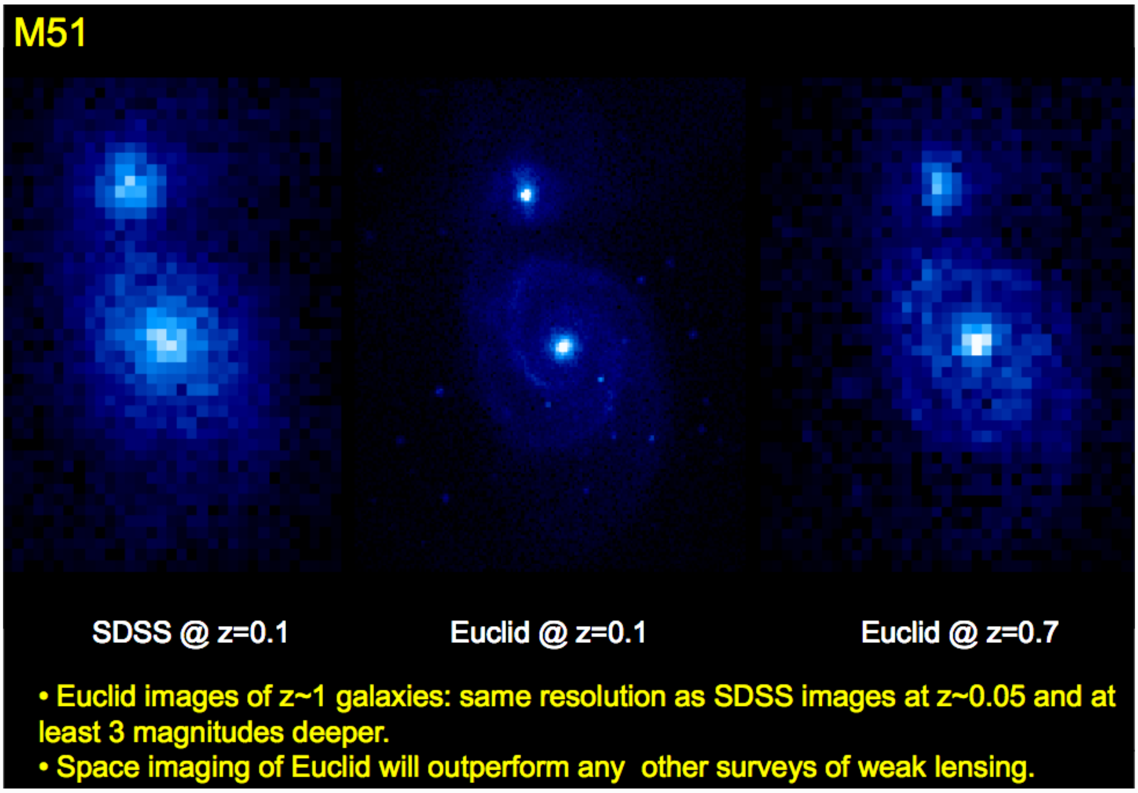

Some Euclid WL challenges

under-sampled PSF

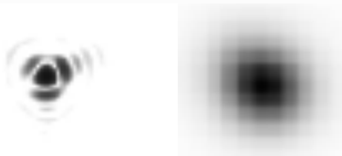

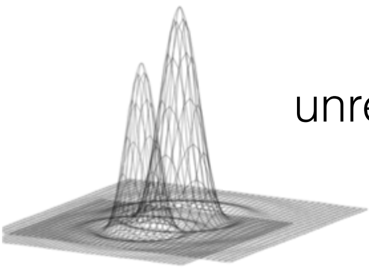

unresolved binary stars

CTI
(charge transfer inefficiency)

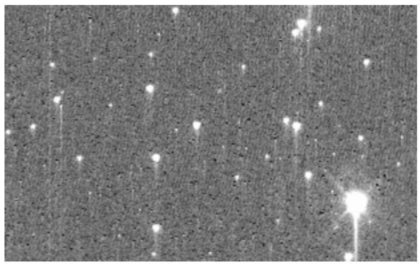

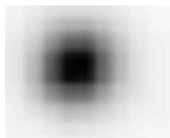

color gradients

Open questions (selection) I

Modelling

- Intrinsic alignment. Dependence on L, type, z? Physically motivated model. N-body simulations.

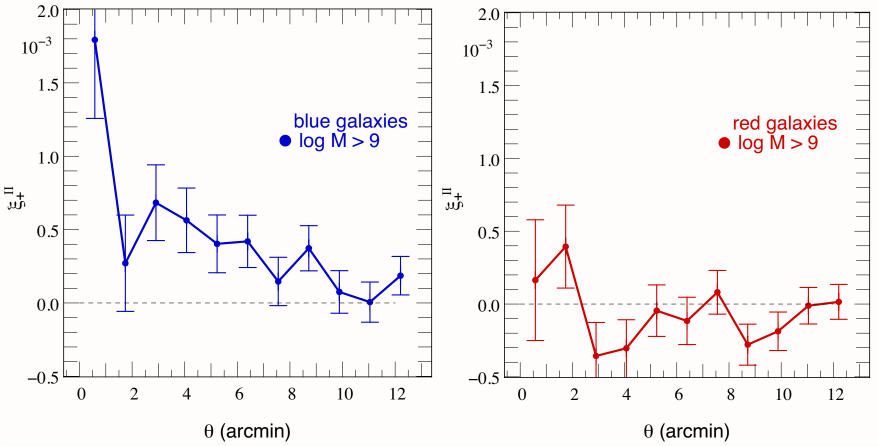

(Codis et al. 2015)

Open questions (selection) II

- IA contamination depends on shape measurement method!

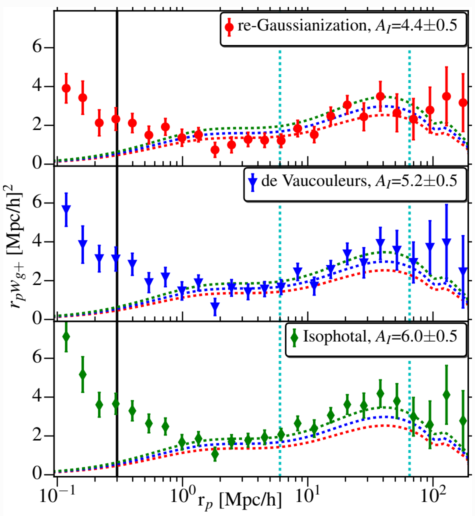

(Singh & Mandelbaum 2016)

Open questions (selection) III

- Baryonic feedback in clusters, influence on WL, modelling.

Photometric redshifts

- Euclid needs (very deep!) ground-based follow-up in multiple optical bands. Data (DES, KiDS, CFIS, ...) will be inhomogeneous. Problem of reliable photo-z's not yet solved.

Further possible topics

1. CMB (x) lensing
2. Cluster weak lensing
3. Nature of dark matter (bullet cluster)
4. Testing GR with WL and galaxy clustering
5. Higher-order statistics: peak counts

CMB (SZ) × WL

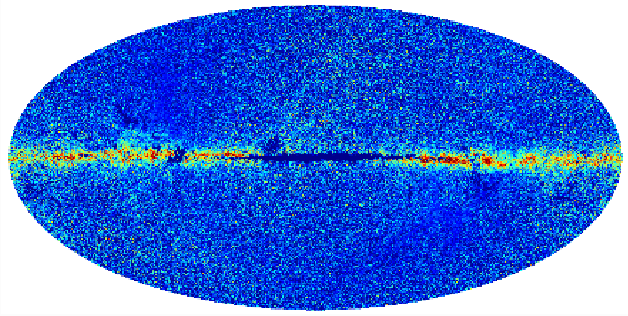

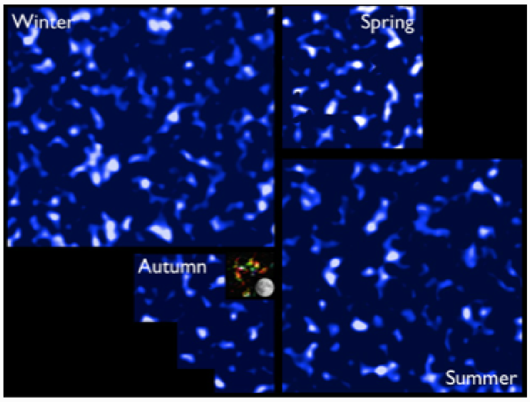

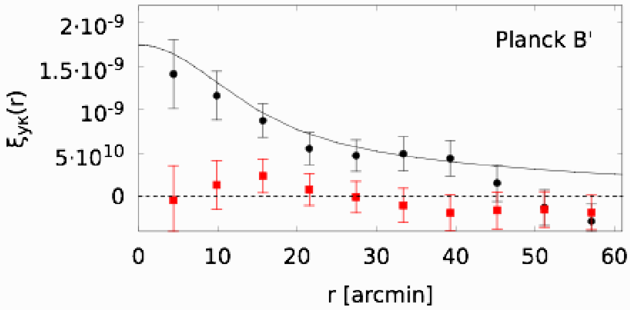

$$\left(\frac{b_{\rm gas}}{1}\right)\left(\frac{T_e(0)}{0.1\ \rm keV}\right)\left(\frac{\bar{n}_e}{1\ \rm m^{-3}}\right) = 2.01 \pm 0.31 \pm 0.21$$

(van Waerbeke et al. 2013b)

Planck CMB (SZ) × CFHTLenS weak-lensing: hot gas associated with matter

CMB lensing

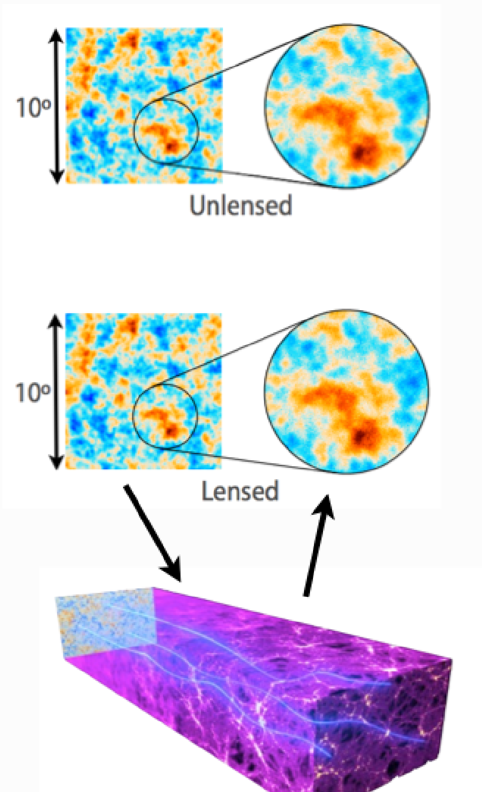

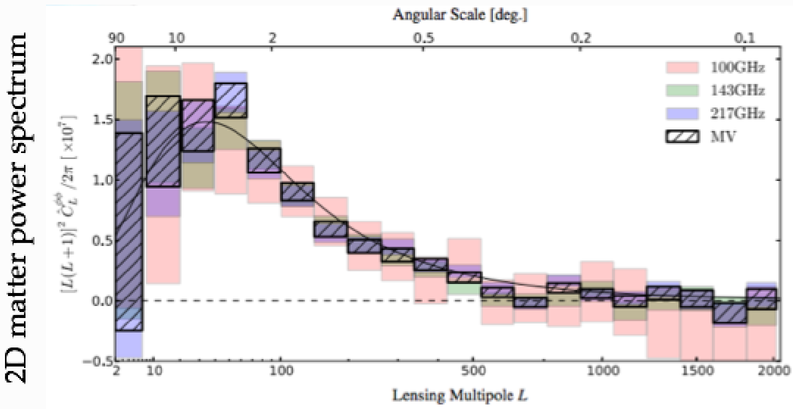

CMB lensing

Béthermin et al. (2013)
Planck Consortium (2014)
Holder et al. (2014)

Planck Consortium (2014)

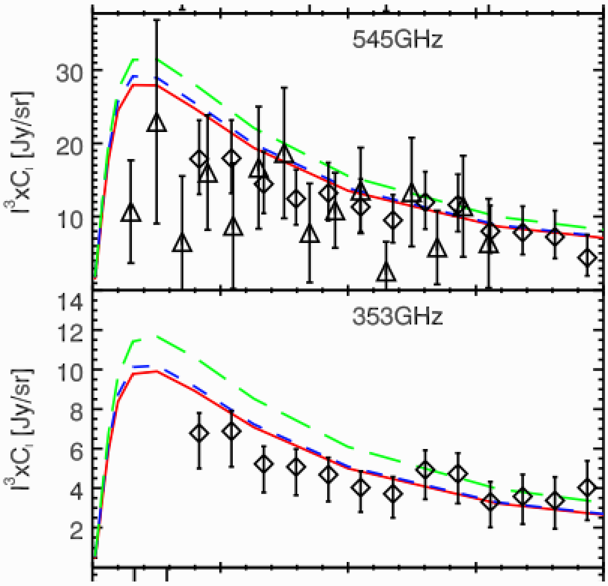

SPT CMB lens x Herschel CIB

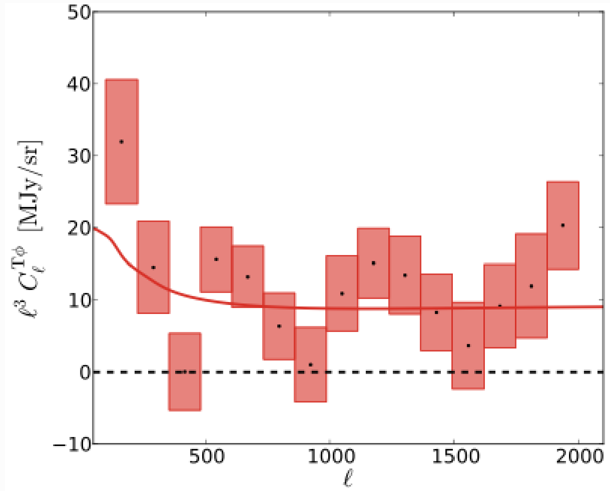

Stacked cluster weak lensing: Large scales

Weak lensing measures mass associated with clusters.

At large distances: excess mass in nearby, correlated clusters
→ clustering of galaxy clusters.

bg shear - fg position ~ $\overline{b_{\rm h}\sigma_8^2}$

halo bias, function of mass

1200 clusters in 150 deg² CFHTLenS area, 0.1 < z < 0.6 (mean z = 0.37).

Covone, Sereno, MK & Cardone (2014)

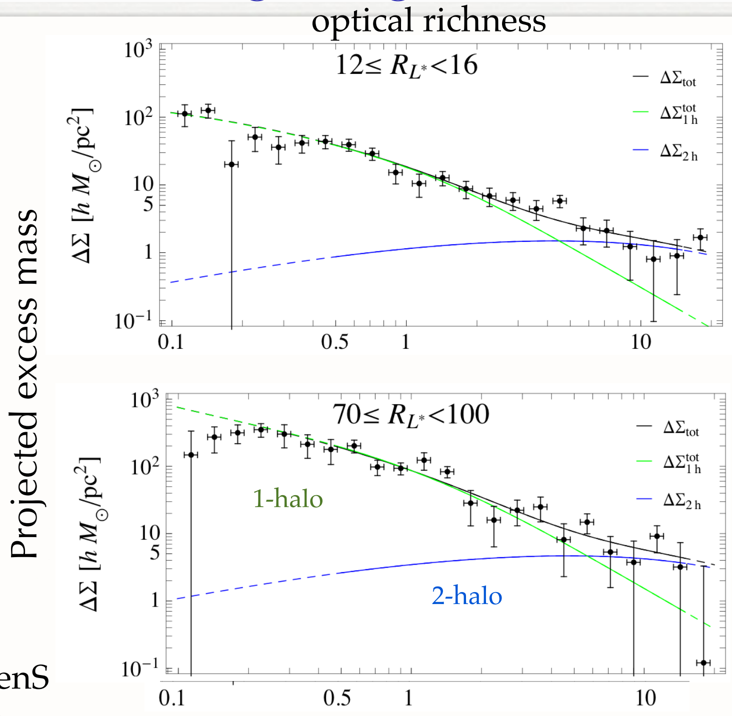

Stacked cluster weak lensing: 2D mass profiles

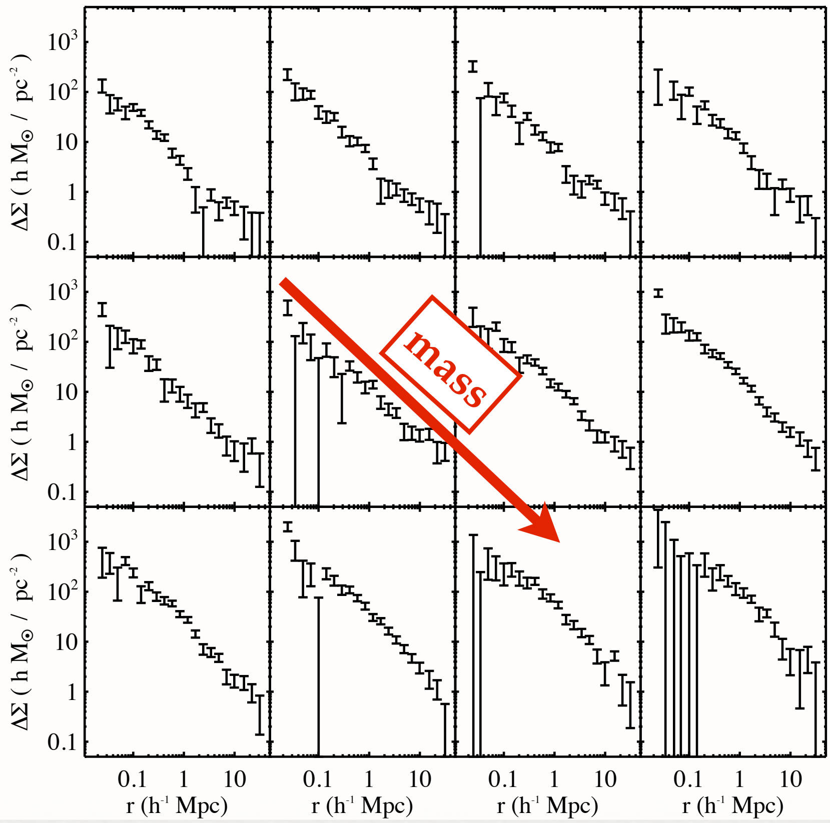

Bin number	N_{200}
1	3
2	4
3	5
4	6
5	7
6	8
7	9-11
8	12-17
9	18-25
10	26-40
11	41-70
12	71-220

130,000 clusters in of SDSS ~ 6,000 deg^2 at z=0.25

Johnston et al. (2009)

Stacked cluster weak lensing: Scaling relations

Covone et al. (2014)

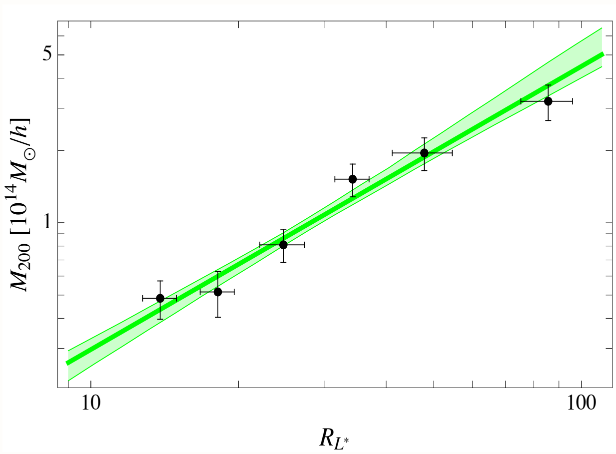

Johnston et al. (2009)

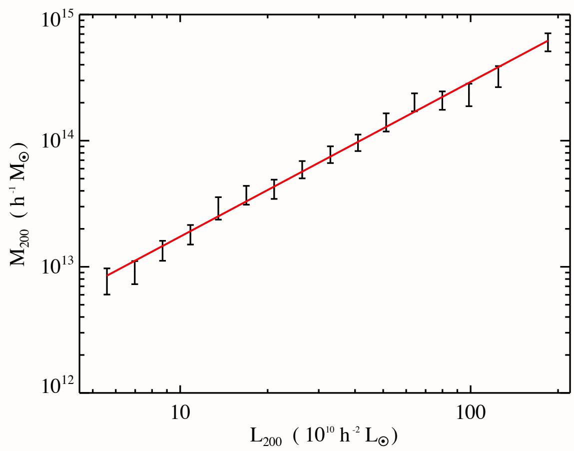

- Scaling relations, necessary calibrating (mass - observable) for cosmology
- XXL (M. Pierre): ~ 100 X-ray selected clusters, 25 deg^2 overlap with CFHTLS, compare lensing and X-ray derived masses.

Stacked cluster weak lensing on large scales

Covone et al. (2014)

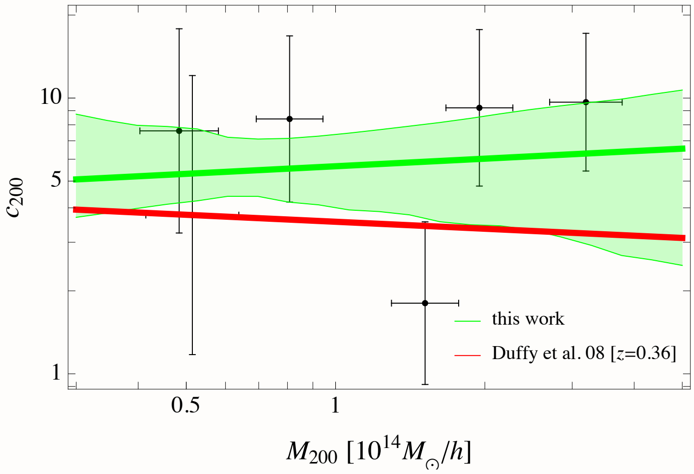

Johnston et al. (2009)

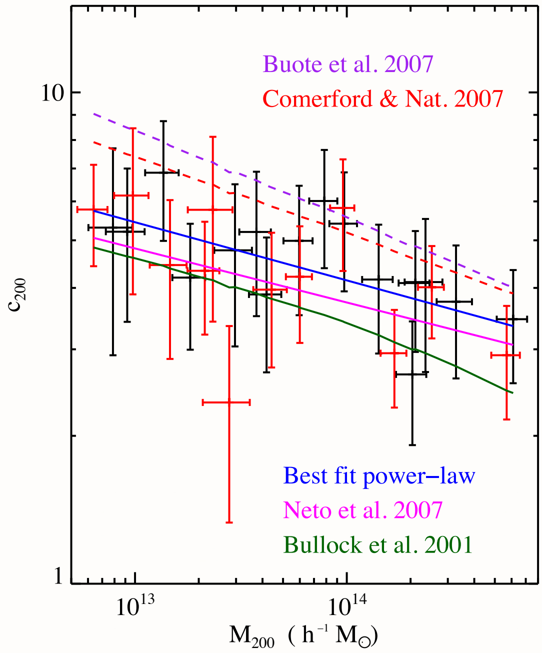

- Concentration parameter c reflects central halo density; depends on assembly history, formation time
- Predictions usually from N-body simulations
- Indirect test of CDM paradigm

The bullet cluster and the nature of dark matter

The bullet cluster

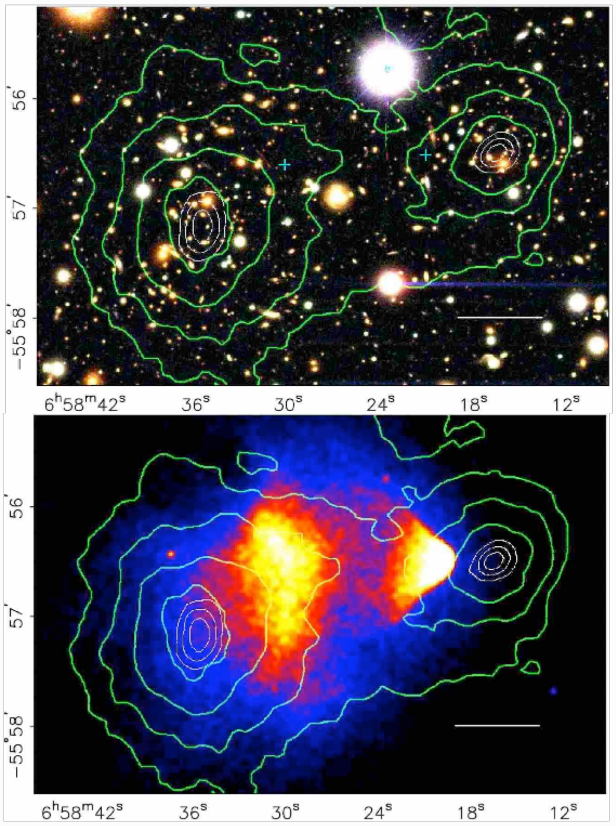

Clowe et al. (2006)

- Merging galaxy cluster at $z = 0.296$
- Recent major merger 100 Myr ago
- Components moving nearly perpendicular to line of sight with $v = 4700$ km s^{-1}
- Galaxy concentration offset from X-ray emission. Bow shocks visible

The bullet cluster: SL+WL measurements

Instrument	Date of Obs.	FoV	Passband	$t_{\rm exp}$ (s)	$m_{\rm lim}$	$n_{\rm d}$ ($'^{-2}$)	seeing
2.2m ESO/MPG	01/2004	$34' \times 34'$	R	14100	23.9	15	0.″8
Wide Field Imager	01/2004		B	6580			1.″0
	01/2004		V	5640			0.″9
6.5m Magellan	01/15/2004	$8'$ radius	R	10800	25.1	35	0.″6
IMACS	01/15/2004		B	2700			0.″9
	01/15/2004		V	2400			0.″8
HST ACS	10/21/2004	3.′5×3.′5	F814W	4944	27.6	87	0.″12
subcluster	10/21/2004		F435W	2420			0.″12
	10/21/2004		F606W	2336			0.″12
main cluster	10/21/2004	3.′5×3.′5	F606W	2336	26.1	54	0.″12

(Bradač et al. 2006, Clowe et al. 2006)

The bullet cluster: strong lensing

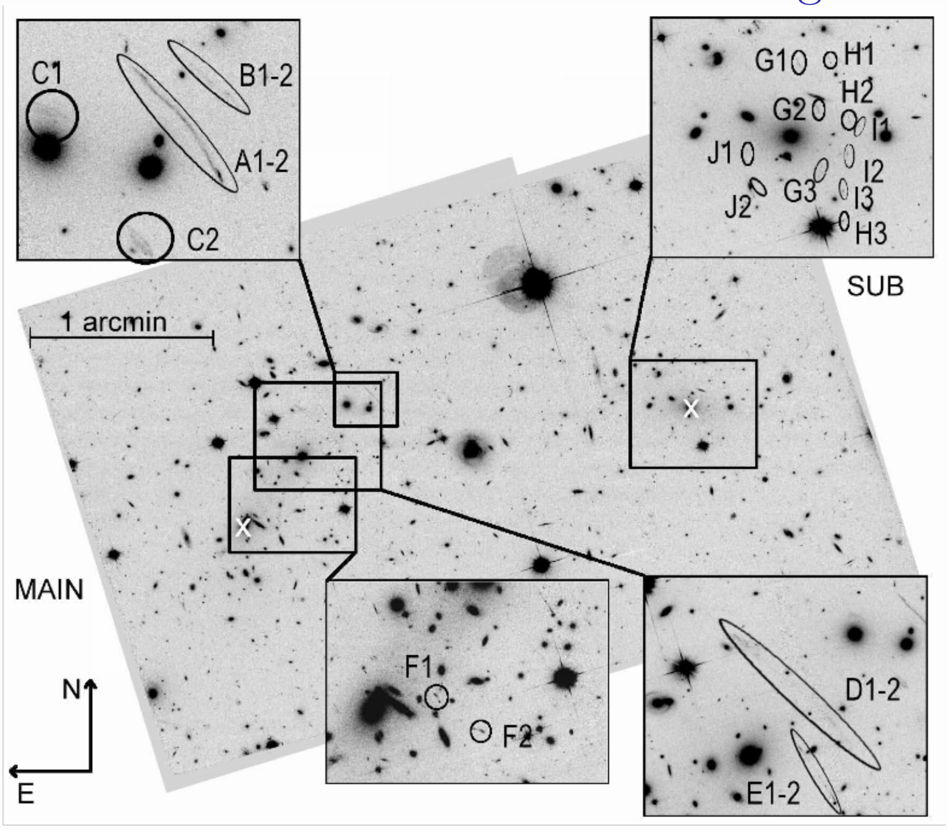

The bullet cluster: WL and X-ray

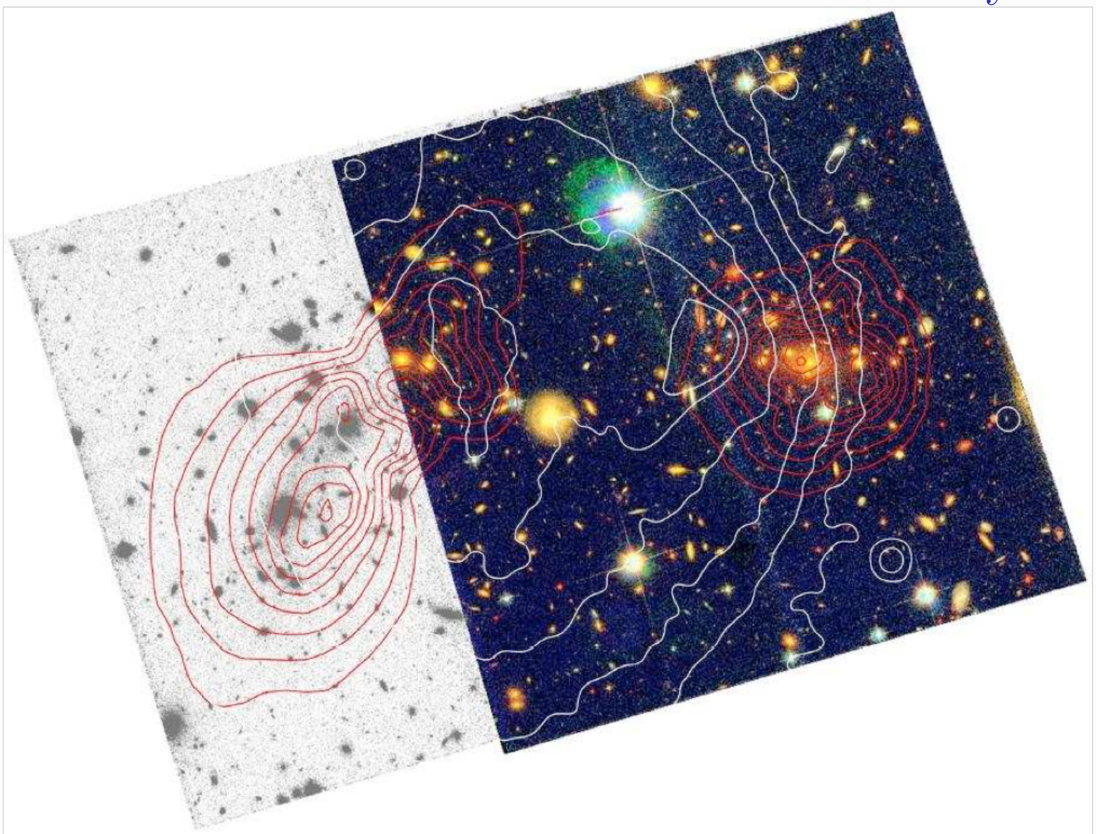

The bullet cluster: Evidence for dark matter

- $10\sigma (6\sigma)$ offset between main (sub-)mass peak and X-ray gas $\to$ most cluster mass is not in hot X-ray gas (unlike most baryonic mass: $m_X \gg m_*$!)
- Main mass associated with galaxies $\to$ this matter is collisionless

Modified gravity theories without dark matter: MoND (Modified Newtonian Dynamics), (Milgrom 1983), changes Newton's law for low accelerations ($a \sim 10^{-10}$ m s^{-2}), can produce flat galaxy rotation curves and Tully-Fisher relation.
MoND's relativistic version (Bekenstein 2004), varying gravitational constant $G(r)$. Introduces new vector field ("phion") with coupling strenght $\alpha(r)$ and range $\lambda(r)$ as free functions.
This can produce non-local weak-lensing convergence mass, where $\kappa \not\propto \delta$!
Necessary to explain offset between main κ peak and main baryonic mass.
Model with four mass peaks can roughly reproduce WL map with additional collisionless mass! E.g. 2 eV neutrinos.

The bullet cluster: MoND model

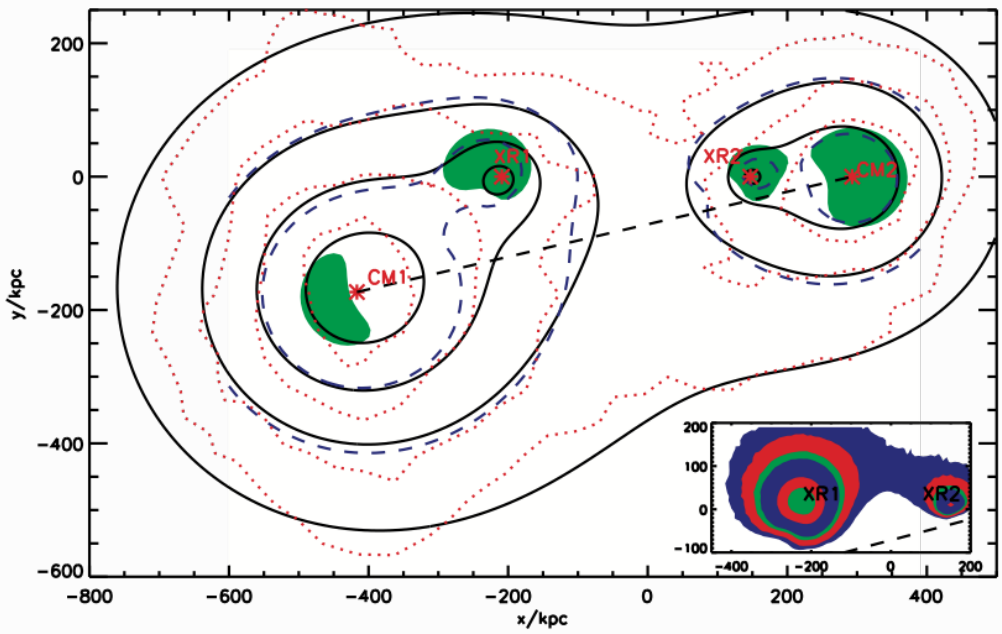

FIG. 1.— Our fitted convergence map (solid black lines) overplotted on the convergence map of C06 (dotted red lines) with x and y axes in kpc. The contours are from the outside 0.16,0.23,0.3 and 0.37. The centres of the four potentials we used are the red stars which are labelled. Also overplotted (blue dashed line) are two contours of surface density $[4.8 \ \& \ 7.2] \times 10^2 M_\odot$ pc^{-2} for the MOND standard μ function; note slight distortions compared to the contours of κ. The green shaded region is where matter density is above $1.8 \times 10^{-3} M_\odot$ pc^{-3} and correspond to the clustering of 2eV neutrinos. *Inset:* The surface density of the gas in the bullet cluster predicted by our collisionless matter subtraction method for the standard μ-function. The contour levels are $[30, 50, 80, 100, 200, 300] M_\odot pc^{-2}$. The origin in RA and dec is $[06^h 58^m 24.38^s, -55^o 56'.32]$

Testing GR with WL and galaxy clustering

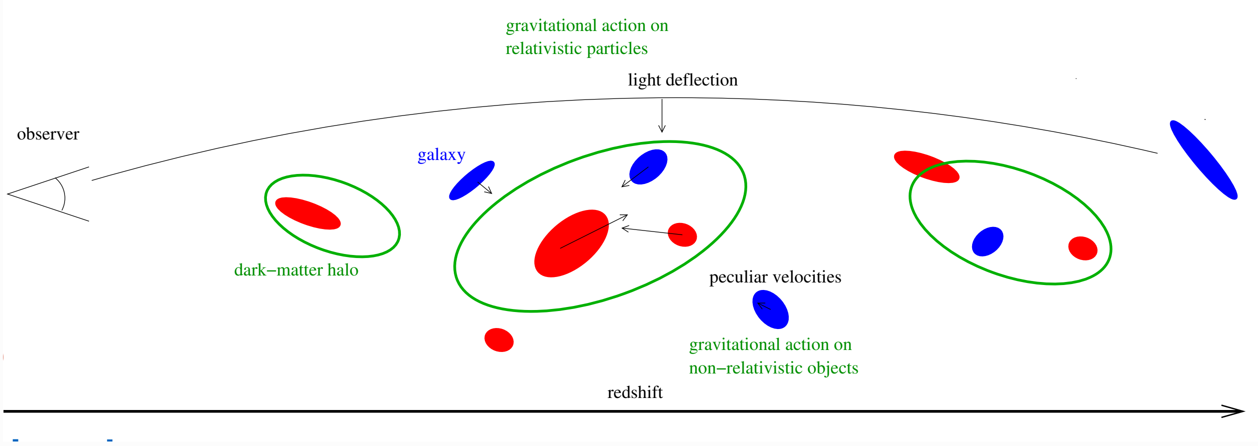

Results from SDSS

SDSS (Reyes et al. 2010)

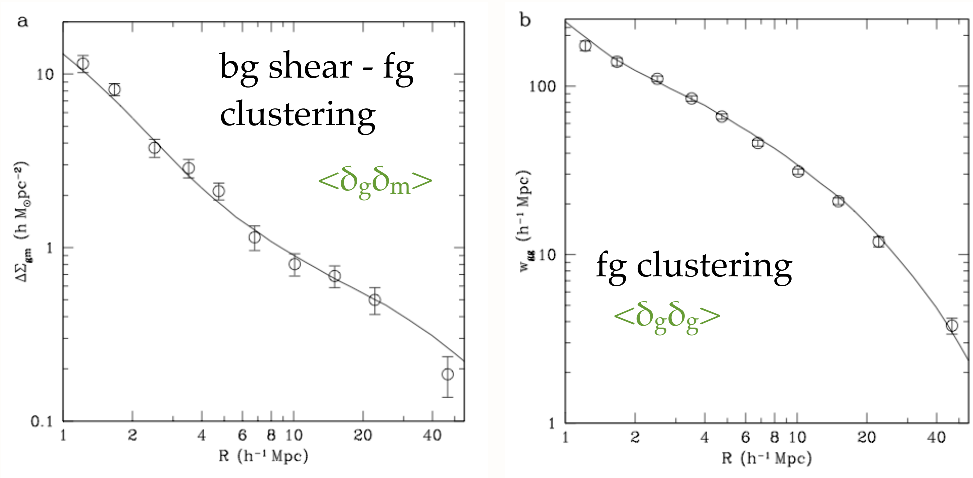

$$E_G \cong \frac{1}{\beta} \frac{\langle \delta_m \delta_g \rangle}{\langle \delta_g \delta_g \rangle}$$

galaxy bias   growth factor

$$\beta = \frac{1}{b} \frac{d \ln D_+}{d \ln a}$$

$\beta = 0.309 \pm 0.035$

from SDSS galaxy clustering (redshift-space distortions) Tegmark et al. (2006)

Results from SDSS

Friedmann-Lemaître-Robertson-Walker metric with perturbations:

$$ds^2 = -(1+2\varphi)dt^2 + (1-2\phi)a^2 dx^2$$

time dilation — spatial curvature

(Reyes et al. 201

- Galaxy-galaxy lensing: measures $\phi + \varphi$ and b
- Galaxy clustering: measures φ

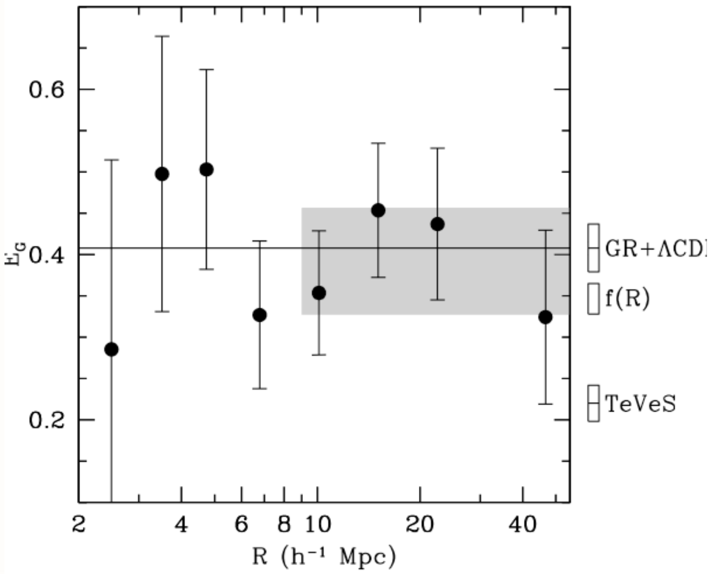

WL peak counts: Why do we want to study peaks?

- WL peaks probe high-density regions ↔ **non-Gaussian** tail of LSS
- **First-order** in observed shear: less sensitive to systematics, circular average!
- High-density regions ↔ **halo mass function**, but **indirect** probe:
  - Intrinsic ellipticity **shape noise**, creating false positives, up-scatter in S/N
  - **Projections** along line of sight

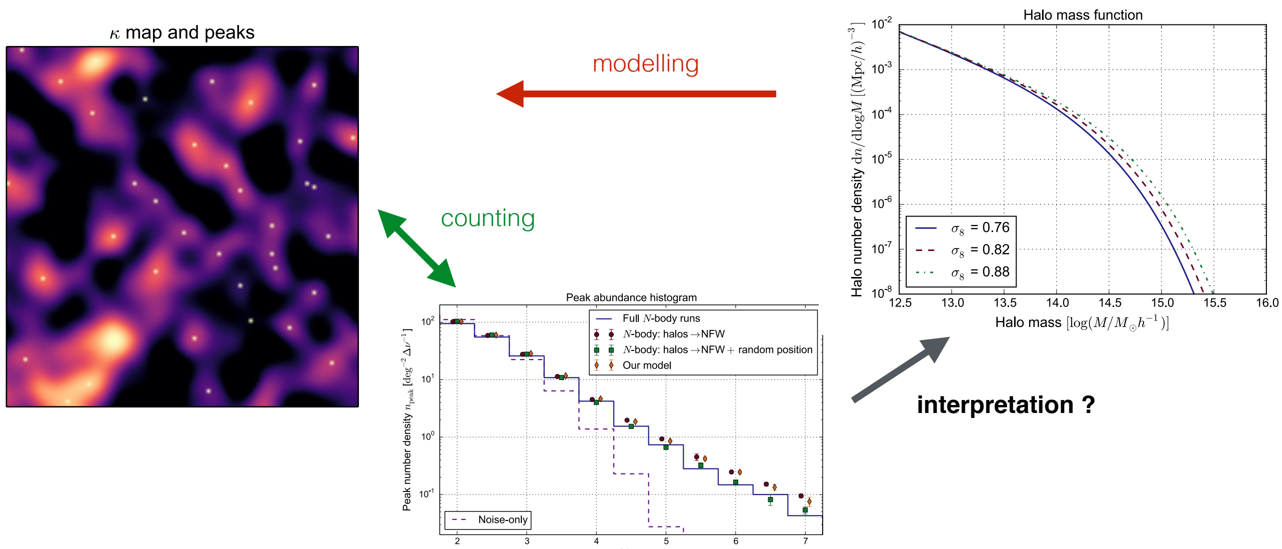

WL peak counts. What are peaks good for?

What do we gain from peak counting?

- Additional and complementary information and constraints compared to 2nd order shear
- Non-Gaussian information

Figure from Dietrich & Hartlap 2010

red/orange: cosmic shear

green: shear & peak

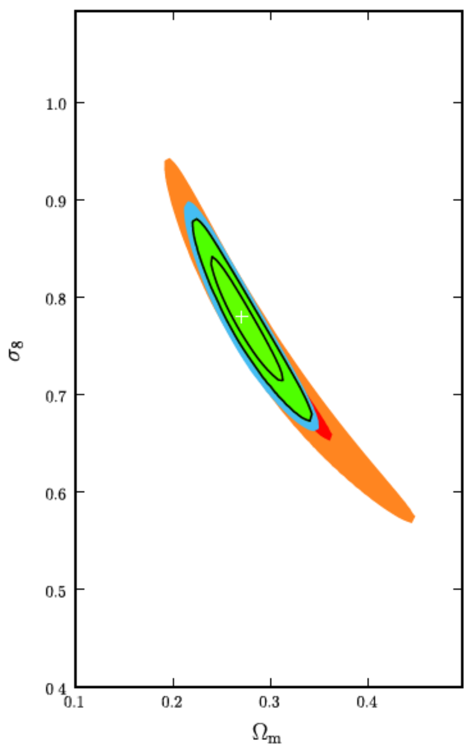

WL peaks: A fast stochastic model

Replace N-body simulations by Poisson distribution of halos

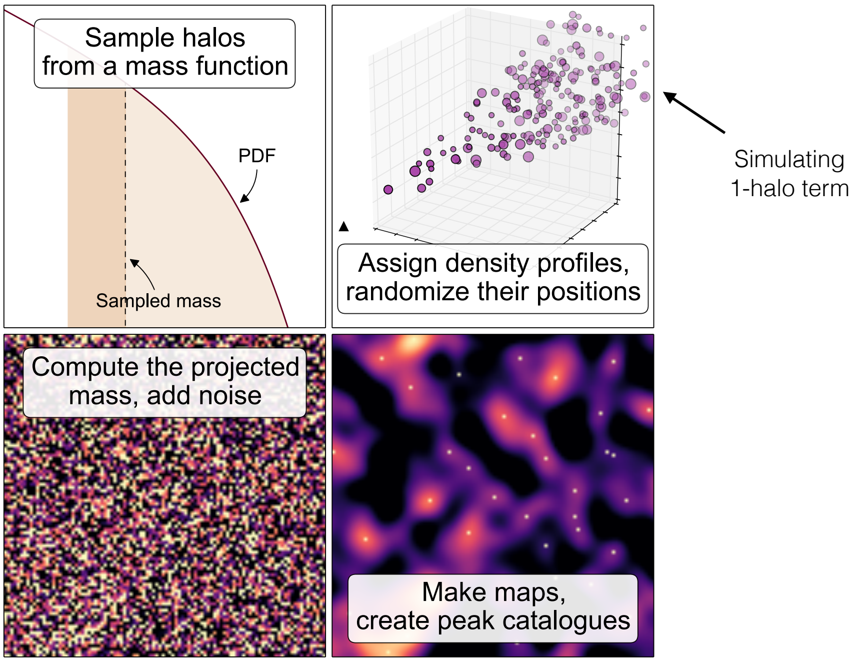

Lin, MK & Pires 2016

WL peaks: histograms

Hypotheses:

1. Clustering of halos not important for counting peaks (along los: Marian et al. 2013)
2. Unbound LSS does not contribute to WL peaks

Test:

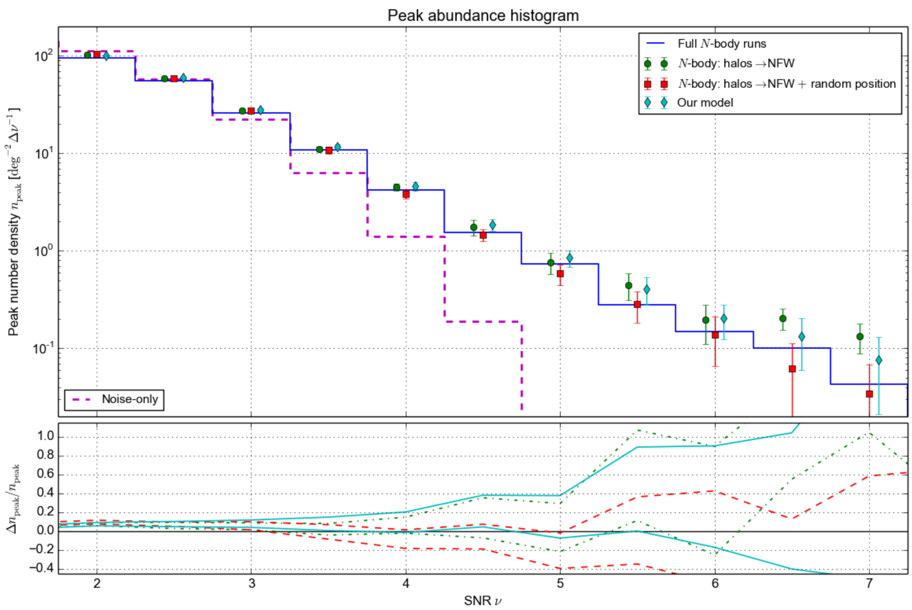

Field of view = 54 deg^2; 10 halo redshift bins from z = 0 to 1; galaxies on regular grid, z_s = 1.0

WL peaks: cosmological parameters

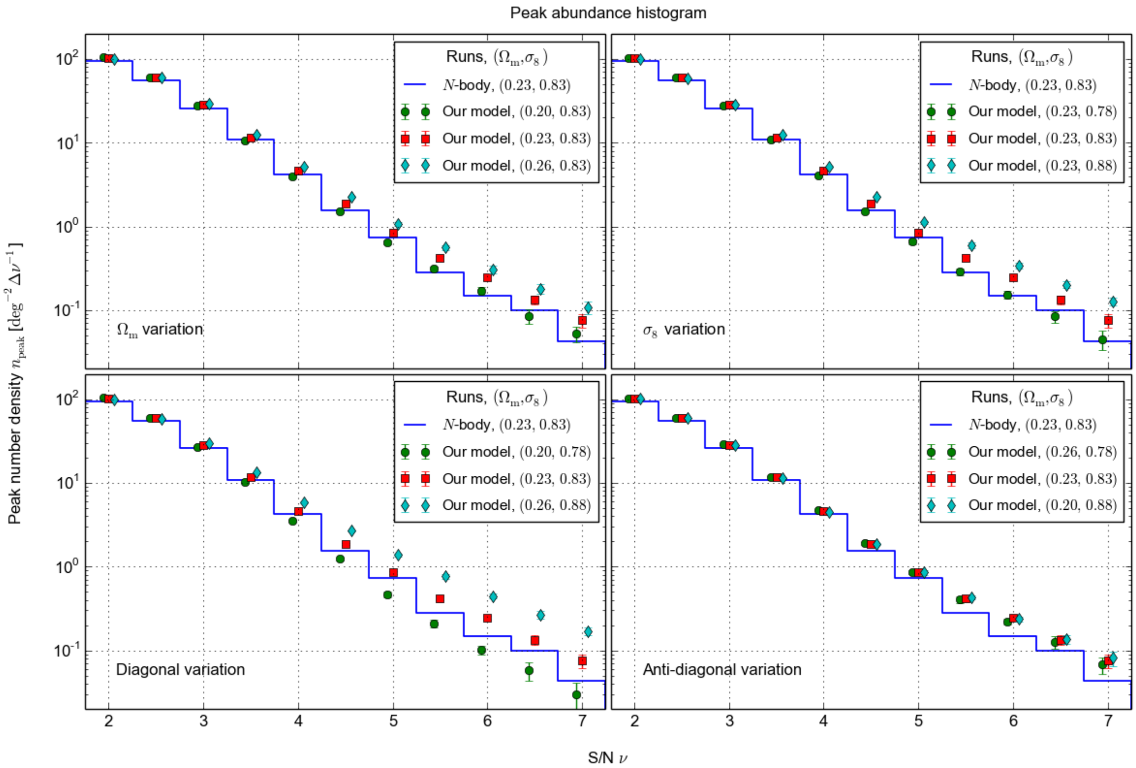

Lin & Kilbinger (2015a)

In general: Constraining cosmological parameters

Bayes' theorem

Likelihood: probability of data given parameters and model

Prior

$$p(\boldsymbol{\pi}|\boldsymbol{x}, m) = \frac{L(\boldsymbol{x}|\boldsymbol{\pi}, m) P(\boldsymbol{\pi}|m)}{E(\boldsymbol{x}|m)}$$

Posterior: probability of parameters given data and model

Evidence

$\boldsymbol{\pi}$: parameters
$\boldsymbol{x}$: data
m : *model*

Parameter constraints = integrals over the posterior

$$\int \mathrm{d}^n\pi \, h(\boldsymbol{\pi}) p(\boldsymbol{\pi}|\boldsymbol{x}, m)$$

For example:

$h(\boldsymbol{\pi}) = \boldsymbol{\pi}$: mean
$h(\boldsymbol{\pi}) = 1_{68\%}$: 68% credible region

Approaches: Sampling (Monte-Carlo integration), Fisher-matrix approximation, frequentist evaluation, ABC, …

WL peaks: data vector choices

Replace N-body simulations by Poisson distribution of halos

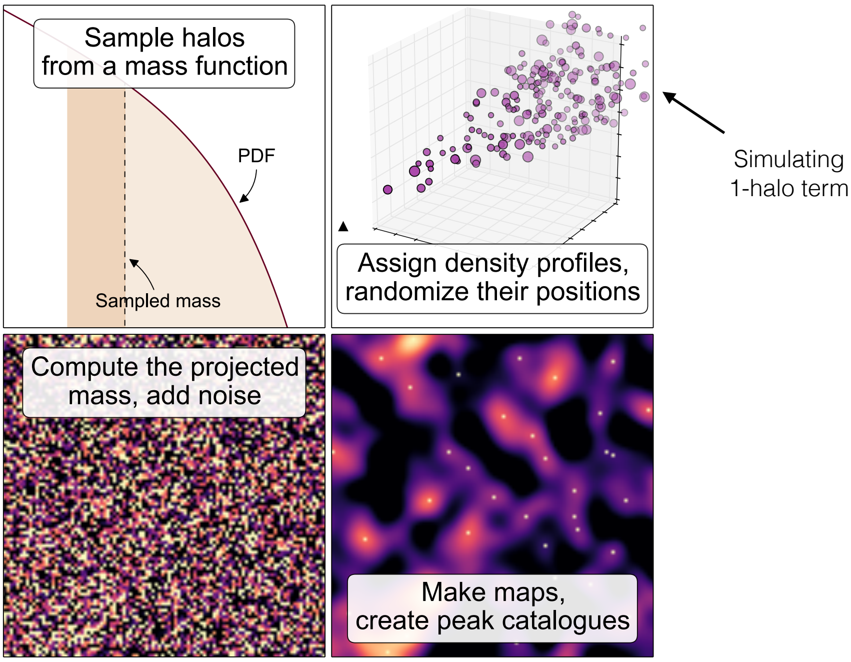

Lin. MK & Pires 2016

WL peaks: Gaussian likelihood

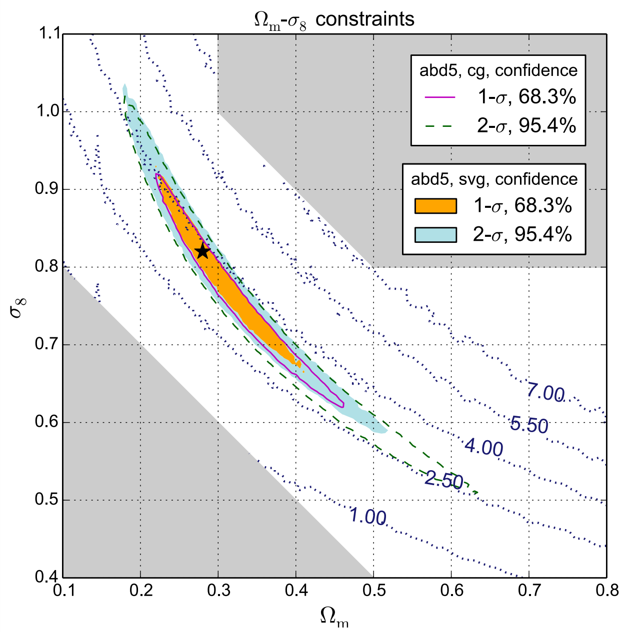

$$L_{\rm cg} \equiv \Delta \boldsymbol{x}^T(\boldsymbol{\pi})\, \widehat{\boldsymbol{C}^{-1}}(\boldsymbol{\pi}^{\rm obs})\, \Delta \boldsymbol{x}(\boldsymbol{\pi}),$$

$$L_{\rm svg} \equiv \Delta \boldsymbol{x}^T(\boldsymbol{\pi})\, \widehat{\boldsymbol{C}^{-1}}(\boldsymbol{\pi})\, \Delta \boldsymbol{x}(\boldsymbol{\pi}), \quad \text{and}$$

$$L_{\rm vg} \equiv \ln\left[\det \widehat{\boldsymbol{C}}(\boldsymbol{\pi})\right] + \Delta \boldsymbol{x}^T(\boldsymbol{\pi})\, \widehat{\boldsymbol{C}^{-1}}(\boldsymbol{\pi})\, \Delta \boldsymbol{x}(\boldsymbol{\pi}).$$

Cosmology-dependent covariance [(s)vg] reduces error area by 20%.

ABC: Approximate Bayesian Computation I

Likelihood:
probability of data given parameters and model

$$p(\boldsymbol{\pi}|\boldsymbol{x}, m) = \frac{L(\boldsymbol{x}|\boldsymbol{\pi}, m) P(\boldsymbol{\pi}|m)}{E(\boldsymbol{x}|m)}$$

$\boldsymbol{\pi}$: parameters
$\boldsymbol{x}$: data
m : model

Likelihood: how likely is it that model prediction $\boldsymbol{x}^{\rm mod}(\boldsymbol{\pi})$ reproduces data $\boldsymbol{x}$?

Classical answer: evaluate function L at $\boldsymbol{x}$.

Alternative: compute fraction of models that are equal to the data $\boldsymbol{x}$.

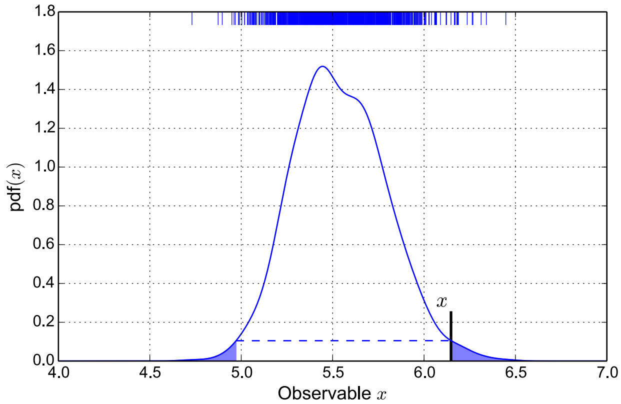

ABC: Approximate Bayesian Computation II

Probability = *p/N* in frequentist sense.

Magic: Don't need to sample *N* models.
One per parameter $\boldsymbol{\pi}$ is sufficient with accept-reject algorithm.

models for given parameter $\boldsymbol{\pi}$

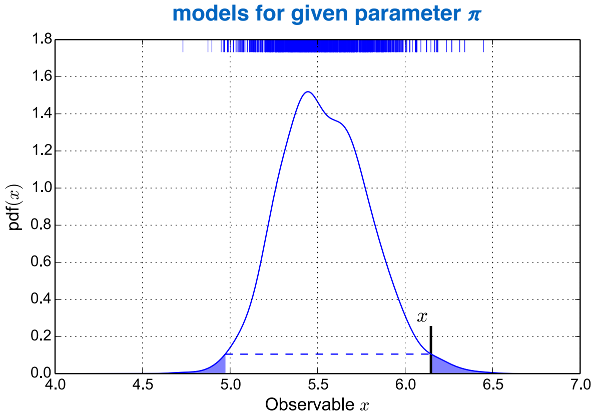

ABC can be performed if:

- it is possible and easy to sample from *L*

ABC is useful when:

- functional form of *L* is unknown
- evaluation of *L* is expensive
- model is intrinsically stochastic

ABC: Approximate Bayesian Computation III

Example: let's make soup.

Goal: Determine ingredients from final result.
Model physical processes? Complicated.

ABC: Approximate Bayesian Computation IV

Example: let's make soup.

Goal: Determine ingredients from final result.
Model physical processes? Complicated.
Easier: Make lots of soups with different ingredients, compare.

ABC: Approximate Bayesian Computation V

Example: let's make soup.

Questions:

- What aspect of data and simulations do we compare? (**summary statistic**)
- How do we compare? (**metric, distance**)
- When do we accept? (**tolerance**)

ABC: Approximate Bayesian Computation VI

Parameter constraints: ABC

- Summary statistic

  $\boldsymbol{s} = \boldsymbol{x}$ (data vector for 2 cases)

- Metric D: two cases

$$D_1\left(\boldsymbol{x}, \boldsymbol{x}^{\text{obs}}\right) \equiv \sqrt{\sum_i \frac{\left(x_i - x_i^{\text{obs}}\right)^2}{C_{ii}}},$$

$$D_2\left(\boldsymbol{x}, \boldsymbol{x}^{\text{obs}}\right) \equiv \sqrt{\left(\boldsymbol{x} - \boldsymbol{x}^{\text{obs}}\right)^T \boldsymbol{C}^{-1} \left(\boldsymbol{x} - \boldsymbol{x}^{\text{obs}}\right)},$$

  D_1 in Lin & MK 2015b

  $D_1 + D_2$ in Lin, MK & Pires 2016

- ABC algorithm: iterative importance sampling (PMC) with decreasing tolerance

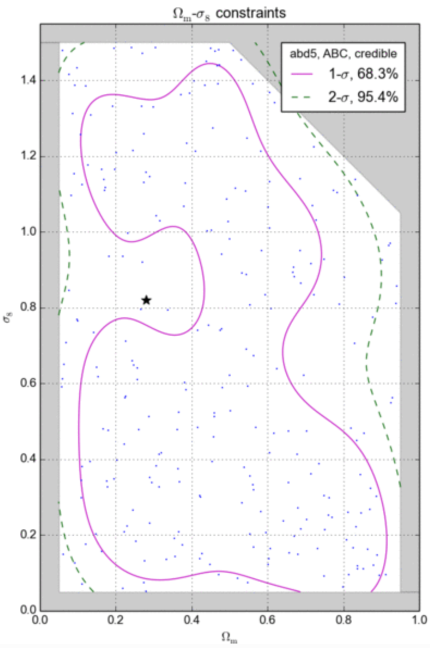

ABC: Approximate Bayesian Computation VII

ABC's accept-reject process is actually a sampling under P_ϵ (green curve):

$$P_\epsilon(\pi|x^{\text{obs}}) = A_\epsilon(\pi)P(\pi),$$

where $P(\pi)$ stands for the prior (blue curve) and

$$A_\epsilon(\pi) \equiv \int \mathrm{d}x\ P(x|\pi)\mathbb{1}_{|x-x^{\text{obs}}|\leq\epsilon}(x),$$

is the accept probability under π (red area). One can see that

$$\lim_{\epsilon\to 0} A_\epsilon(\pi_0)/\epsilon = P(x^{\text{obs}}|\pi_0) = \mathcal{L}(\pi_0),$$

so P_ϵ is proportional to the true posterior when $\epsilon \to 0$.

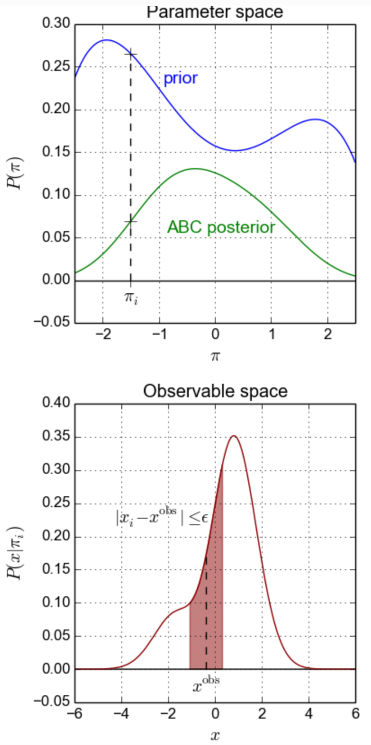

ABC: Approximate Bayesian Computation VIII

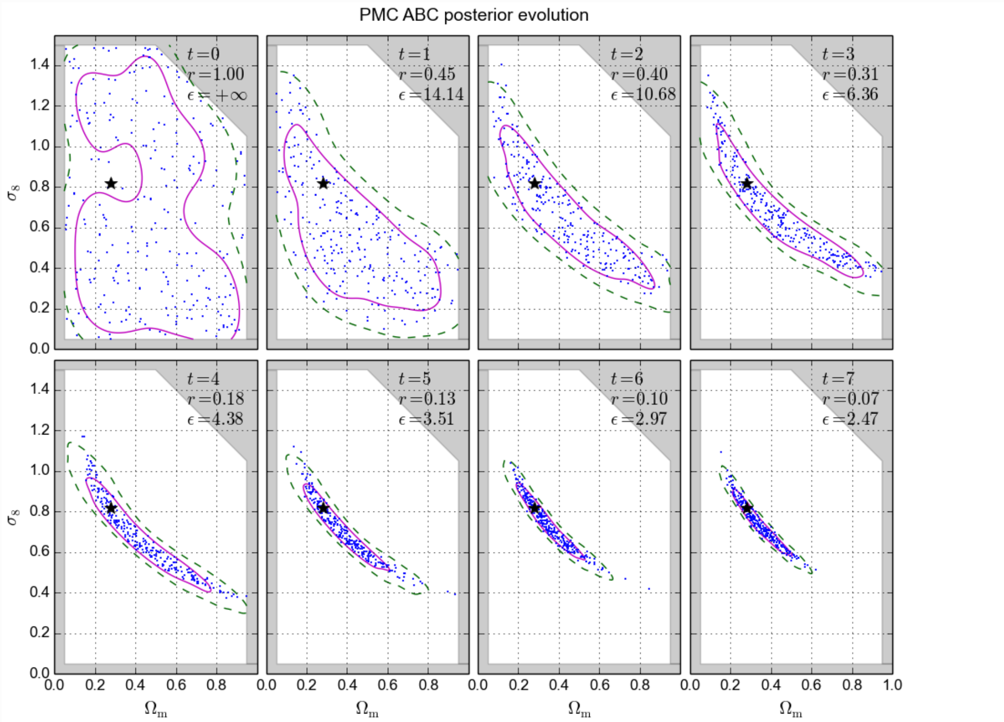

Lin & Kilbinger (2015b)

ABC: Approximate Bayesian Computation IX

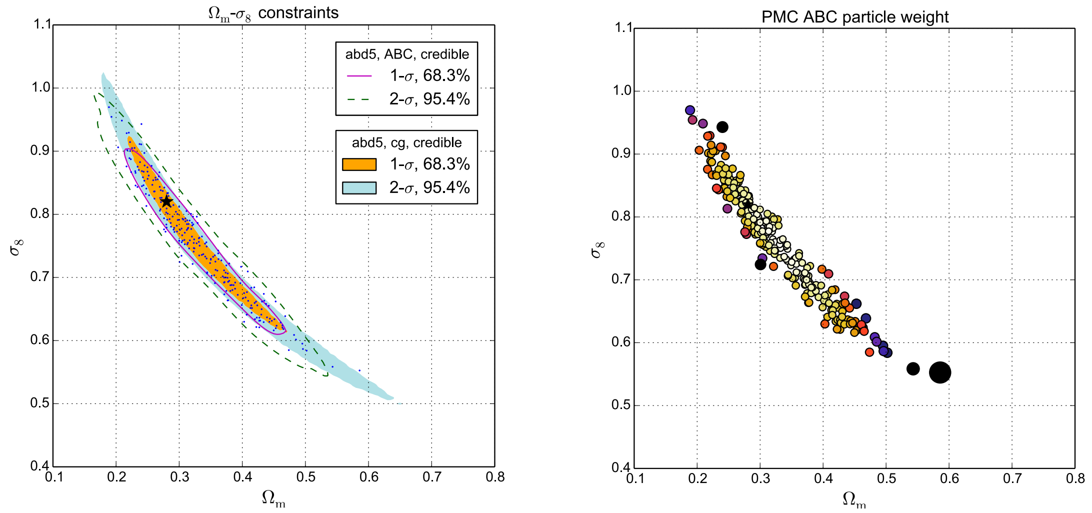

ABC wider but less elongated and less bent contours than Gaussian with const cov. KDE smoothing effect?

Bibliography I

Beaulieu J P, Bennett D P, Fouqué P, Williams A, Dominik M & al. 2006 *Nature* **439**, 437–440.

Bekenstein J D 2004 *Phys. Rev. D* **70**(8), 083509.

Benítez N 2000 *ApJ* **536**, 571–583.

Bernstein G M & Armstrong R 2014 *MNRAS* **438**, 1880–1893.

Bolzonella M, Miralles J M & Pelló R 2000 *A&A* **363**, 476–492.

Bonamente M, Hasler N, Bulbul E, Carlstrom J E, Culverhouse T L & al. 2012 *New Journal of Physics* **14**(2), 025010.
URL: *http://stacks.iop.org/1367-2630/14/i=2/a=025010*

Bradač M, Clowe D, Gonzalez A H, Marshall P, Forman W & al. 2006 *ApJ* **652**, 937–947.

Clowe D, Bradač M, Gonzalez A H, Markevitch M, Randall S W & al. 2006 *ApJ* **648**, L109–L113.

Codis S, Gavazzi R, Dubois Y, Pichon C, Benabed K & al. 2015 *MNRAS* **448**, 3391–3404.

Bibliography II

Collister A A & Lahav O 2004 *PASP* **116**, 345–351.

Gentile M, Courbin F & Meylan G 2012 *arXiv:1211.4847* .

Gentile M, Courbin F & Meylan G 2013 *A&A* **549**, A1.

Heymans C, Grocutt E, Heavens A, Kilbinger M, Kitching T D & al. 2013 *MNRAS* **432**, 2433–2453.

Heymans C, Van Waerbeke L, Miller L, Erben T, Hildebrandt H & al. 2012 *MNRAS* **427**, 146–166.

Hildebrandt H, Viola M, Heymans C, Joudaki S, Kuijken K & al. 2017 *MNRAS* **465**, 1454–1498.

Hirata C M, Mandelbaum R, Ishak M, Seljak U, Nichol R & al. 2007 *MNRAS* **381**, 1197–1218.

Hirata C M & Seljak U 2004 *Phys. Rev. D* **70**(6), 063526–+.

Hoag A, Bradac M, Trenti M, Treu T, Schmidt K B & al. 2017 *Nature Astronomy* **1**, 0091.

Huterer D, Takada M, Bernstein G & Jain B 2006 *MNRAS* **366**, 101–114.

Bibliography III

Ilbert O, Arnouts S, McCracken H J, Bolzonella M, Bertin E & al. 2006 *A&A* **457**, 841–856.

Jarvis M, Sheldon E, Zuntz J, Kacprzak T, Bridle S L & al. 2016 *MNRAS* **460**, 2245–2281.

Joachimi B, Cacciato M, Kitching T D, Leonard A, Mandelbaum R & al. 2015 *Space Sci. Rev.* **193**, 1–65.

Kaiser N, Squires G & Broadhurst T 1995 *ApJ* **449**, 460.

Kilbinger M, Fu L, Heymans C, Simpson F, Benjamin J & al. 2013 *MNRAS* **430**, 2200–2220.

Kuijken K 1999 *A&A* **352**, 355–362.

Kuijken K 2006 *A&A* **456**, 827–838.

Lima M, Cunha C E, Oyaizu H, Frieman J, Lin H & al. 2008 *MNRAS* **390**, 118–130.

Massey R & Refregier A 2005 *MNRAS* **363**, 197–210.

Melchior P, Viola M, Schäfer B M & Bartelmann M 2011 *MNRAS* **412**, 1552–1558.

Milgrom M 1983 *Astrophysical Journal* **270**, 371–389.

Bibliography IV

Miller L, Kitching T D, Heymans C, Heavens A F & van Waerbeke L 2007 *MNRAS* **382**, 315–324.

Okura Y & Futamase T 2009 *ApJ* **699**, 143–149.

Planck Collaboration, Ade P A R, Aghanim N, Armitage-Caplan C, Arnaud M & al. 2014 *A&A* **571**, A17.

Refregier A 2003 *MNRAS* **338**, 35–47.

Reyes R, Mandelbaum R, Seljak U, Baldauf T, Gunn J E & al. 2010 *Nature* **464**, 256–258.

Schneider M D, Hogg D W, Marshall P J, Dawson W A, Meyers J & al. 2014 *ArXiv e-prints* .

Semboloni E, Hoekstra H, Schaye J, van Daalen M P & McCarthy I G 2011 *MNRAS* **417**, 2020–2035.

Simpson F, Heymans C, Parkinson D, Blake C, Kilbinger M & al. 2013 *MNRAS* **429**, 2249–2263.

Singh S & Mandelbaum R 2016 *MNRAS* **457**, 2301–2317.

Bibliography V

Tewes M, Cantale N, Courbin F, Kitching T & Meylan G 2012 *A&A* **544**, A8.

The Dark Energy Survey Collaboration, Abbott T, Abdalla F B, Allam S, Amara A & al. 2016 *Phys. Rev. D* **94**, 022001.

Van Waerbeke L, Mellier Y, Erben T, Cuillandre J C, Bernardeau F & al. 2000 *A&A* **358**, 30–44.

Velander M, van Uitert E, Hoekstra H, Coupon J, Erben T & al. 2014 *MNRAS* **437**, 2111–2136.

von der Linden A, Allen M T, Applegate D E, Kelly P L, Allen S W & al. 2014 *MNRAS* **439**, 2–27.

Walsh D, Carswell R F & Weymann R J 1979 *Nature* **279**, 381–384.

Zuntz J, Kacprzak T, Voigt L, Hirsch M, Rowe B & al. 2013 *MNRAS* **434**, 1604–1618.